

# From Microscopic Compartmentalization to Hydrodynamic Patterns: New Pathways for Information Transport

Marcello A. Budroni<sup>1</sup>(✉), Jorge Carballido-Landeira<sup>2</sup>, Adriano Intiso<sup>3</sup>,  
Lorena Lemaigre<sup>2</sup>, Anne De Wit<sup>2</sup>, and Federico Rossi<sup>3</sup>(✉)

<sup>1</sup> Department of Chemistry and Pharmacy, University of Sassari, Sassari, Italy  
mabudroni@uniss.it

<sup>2</sup> Nonlinear Physical Chemistry Unit, Service de Chimie Physique et Biologie  
Théorique, Université libre de Bruxelles, CP 231 - Campus Plaine,  
1050 Brussels, Belgium

<sup>3</sup> Department of Chemistry and Biology, University of Salerno,  
via Giovanni Paolo II 132, 84084 Fisciano, SA, Italy

frossi@unisa.it

<http://physchem.uniss.it/cnl.dyn/budroni.html>,

<http://www.unisa.it/docenti/federicorossi/index>

**Abstract.** Can we exploit hydrodynamic instabilities to trigger an efficient, selective and spontaneous flow of encapsulated chemical information? One possible answer to this question is presented in this paper where cross-diffusion, which commonly characterizes compartmentalized dispersed systems, is shown to initiate buoyancy-driven hydrodynamic instabilities. A general theoretical framework allows us to predict and classify cross-diffusion-induced convection in two-layer stratifications under the action of the gravitational field. The related nonlinear dynamics is described by a cross-diffusion-convection (CDC) model where fickian diffusion is coupled to the Stokes equations. We identify two types of hydrodynamic modes (the negative cross-diffusion-driven convection, NCC, and the positive cross-diffusion-driven convection, PCC) corresponding to the sign of the cross-diffusion term dominating the system dynamics. We finally show how AOT water-in-oil reverse microemulsions are an ideal model system to confirm the general theory and to approach experimentally cross-diffusion-induced hydrodynamic scenarios.

**Keywords:** Transport of chemical information · Compartmentalization · Water-in-oil reverse microemulsions · Buoyancy-driven instabilities · Cross-diffusion · Multi-components systems

## 1 Introduction

The compartmentalization of chemical systems plays a central role in generating unexpected novelties and emergent dynamical behaviors. Many self-assembled matrices including micelles [11, 12], lipid vesicles [20] and microemulsions [25]

have been extensively studied as model systems for mimicking biological cellular environments and related complex intra- and inter-dynamics. The spatial confinement of chemical species can affect the global dynamics of a system by changing drastically the diffusive transport inside and across the confined domains and also inducing a catalytic effect in the chemical reactivity [22]. For these characteristics, dispersed media have often been studied in combination with nonlinear oscillatory kinetics to approach collective behaviors, communication and synchronization dynamics in networks of coupled inorganic oscillators [6, 13, 16, 19, 21].

In this context, the AOT (sodium bis(2-ethylhexyl)sulfosuccinate Aerosol OT) water-in-oil reverse microemulsions (ME) are one of the most investigated systems. ME are liquid mixtures of an organic solvent (more often termed oil) in which water domains surrounded by a surfactant (AOT) can form a thermodynamically stable dispersion (see Fig. 1). In particular, under the percolation threshold, ME appear at the nano-scale as dispersed spherical or elongated droplets where the surfactant constitutes a sort of membrane with the hydrophobic part oriented towards the outer organic phase and the hydrophilic heads in contact with the inner aqueous phase segregated into the droplet. In this situation, the water core of the ME can be conveniently used to dissolve hydrophilic molecules or reactants and become a suitable tool for nano-synthesis, drug delivery or for studying chemical communication [6, 8]. The oscillatory Belousov-Zhabotinsky (BZ) reaction has been thoroughly studied in ME. Here BZ reagents are solubilized in the water core of AOT-coated nano-droplets to create a great amount of nano-oscillators, which dynamics is coupled *via* some active intermediates of the BZ system able to cross the hydrophobic membrane of the surfactant and act as messengers among the confined water domains. Microemulsions are also important in the realm of reaction-diffusion-driven pattern formation. Turing structures and other exotic dissipative structures have been found when ME, loaded with reactants of the BZ system, are studied in spatially extended reactors [7, 24]. Thanks to the selective permeability of the surfactant barrier with regard to the BZ species, this system sustains differential diffusion and can meet the requirements for a Turing instability with the slow diffusion mode involving the activator of the BZ oscillator (which moves with the droplets), while the hydrophobic inhibitor, free to move alone through both the oil and the aqueous phase, presents a diffusion coefficient two orders of magnitude larger than the activator.

Cross-diffusion, whereby a flux of a given species entrains the diffusive transport of another species, is also an important process which takes place in ME systems. Measurements of cross-diffusion coefficients in ternary AOT microemulsions (H<sub>2</sub>O (1)/AOT (2)/oil) revealed that the cross-diffusion coefficient  $D_{12}$ , which describes the flux of water induced by a gradient in the surfactant concentration, can be significantly larger than both  $D_{11}$  and  $D_{22}$ , i.e. the main diffusion coefficients of water and AOT, respectively [9, 10]. The crucial influence of cross-diffusive contributions in terms of pattern formation has been proved in non-reactive and reactive spatially distributed systems, both theoretically [26, 27] and experimentally [4, 14]. Thus, the constraints imposed to diffusive transport

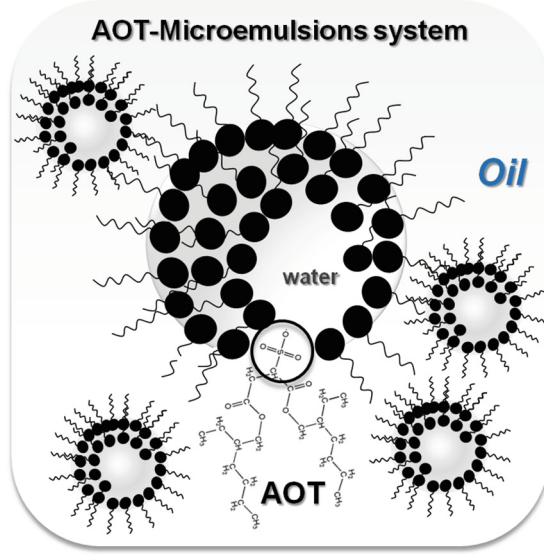


Fig. 1. Sketch of AOT water-in-oil reverse microemulsions.

by compartmentalization at a microscopic scale impact emergent behaviors at a macroscopic characteristic length. Apart for reaction-diffusion patterns, such variety of diffusive modes can trigger hydrodynamic instabilities, when buoyancy forces are at play [23]. Convection is the most efficient spontaneous transport mechanism and can be suitably engineered to enhance spatial spreading of chemical information encapsulated into droplets in response to initial concentration gradients.

With this perspective, we review our recent work where ME are presented as a convenient model system for inducing cross-diffusion-driven hydrodynamic flows in double-layer systems. We first present a general modeling and theory on buoyancy-driven convection promoted by cross-diffusion and we successively study experimentally convective patterns occurring when two ME are stratified in a Hele-Shaw cell [2, 3].

## 2 Theory

Consider a two dimensional vertical slab of width  $L_X$  and height  $L_Z$  in a  $(X, Z)$  reference frame, where the gravitational acceleration  $\bar{g} = (0, -g)$  is oriented downwards along the  $Z$  axis. The solution  $T$  of density  $\rho^T$ , containing the solute  $h$  with the initial concentration  $C_{h,0}^T$  and the solute  $j$  with concentration  $C_{j,0}^T$  is placed on top of the solution  $B$ , with concentration  $C_{h,0}^B = C_{h,0}^T$ ,  $C_{j,0}^B > C_{j,0}^T$  and density  $\rho^B > \rho^T$  (see sketch in Fig. 2). In other words, the species  $h$  is homogeneously distributed over the spatial domain, while the concentration of the species  $j$  increases downwards the gravitational axis.

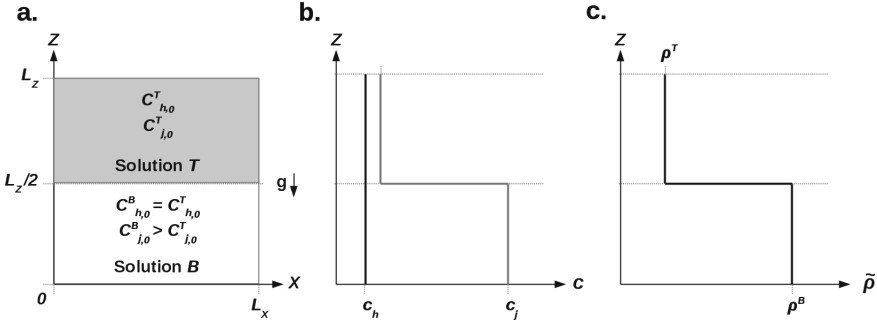


**Fig. 2.** Sketch of the two-dimensional initial stratification used to study cross-diffusion-driven convection. The initial concentration profiles of the chemical solutes result in a step function density distribution.

The resulting double-layer stratification is stable to classical Rayleigh-Taylor or buoyancy-driven instabilities due to differential diffusion mechanisms, such as double-diffusion or double-layer-convection scenarios, and thus it is ideal to isolate the pure effect of cross-diffusion on the system stability.

Before the onset of an instability, we can assume that the flow is at rest and that the concentration profiles of the species do not vary along the horizontal  $x$  direction. The initial evolution of the concentration fields can be thus followed along the vertical coordinate  $z$  and described by means of the dimensionless cross-diffusion equations

$$\partial_\tau c_j = \nabla^2 c_j + \delta_{jh} \nabla^2 c_h \tag{1}$$

$$\partial_\tau c_h = \delta_{hj} \nabla^2 c_j + \delta_{hh} \nabla^2 c_h \tag{2}$$

where the spatial and the time variables are scaled by  $L_0$  and  $t_0 = L_0^2/D_{jj}$ , respectively and  $D_{jj}$  is the dimensional main diffusivity of the heterogeneously distributed species. The concentration fields are non-dimensionalized by the reference  $\Delta C_{j,0} = (C_{j,0}^B - C_{j,0}^T)$  according to  $(c_j, c_h) = (C_j - C_{j,0}^T, C_h - C_{h,0}^T)/\Delta C_{j,0}$ , and  $\delta_{hh} = D_{hh}/D_{jj}$  is the ratio between the main molecular diffusion coefficient of solute  $h$  to that of  $j$ . Similarly,  $(\delta_{jh}, \delta_{hj}) = (D_{jh}, D_{hj})/D_{jj}$ .

Possible cross-diffusion feedbacks on the dynamics are measured in the matrix  $\delta$  and, in particular, due to the sharp initial gradient imposed to the concentration profile  $c_j(z, 0)$ , the off-diagonal term  $\delta_{hj}$  dominates the initial part of the dynamics while the other cross-diffusivity,  $\delta_{jh}$ , plays a negligible role. If  $\delta_{hj}$  is positive, the species  $j$ , free to diffuse from the bottom to the upper layer in response to its initial concentration gradient (Fig. 3(a)), generates a co-flux in  $h$  and, as a result, the initially flat concentration profile  $c_h(z, \tau)$  develops a non-monotonic shape with a local maximum and minimum symmetrically located above and below the initial interface, respectively (Fig. 3(b)). By contrast, the propagation of solute  $j$  towards the upper layer triggers a counter-flux in  $h$  if  $\delta_{hj}$  is negative. In the concentration profile  $c_h(z, \tau)$  this produces in time a local

depletion area in the upper layer and an accumulation just below the initial interface located at  $z_0 = L_Z/(2L_0)$  (Fig. 3(d–e)). We clearly observe an inversion in the morphology of the non-monotonic profiles when switching from a positive to a negative  $\delta_{hj}$  and the relative intensity of the extrema along the non-monotonic profiles reflects the magnitude of this term.

The non-monotonic concentration profiles triggered by cross-diffusion in species  $h$  can drastically impact the density distribution along the gravitational axis. The density profile can be computed as a Taylor expansion of the concentration fields according to

$$\rho(z, \tau) = c_j(z, \tau) + R c_h(z, \tau) \quad (3)$$

where the buoyancy ratio

$$R = \frac{\alpha_h}{\alpha_j} \quad (4)$$

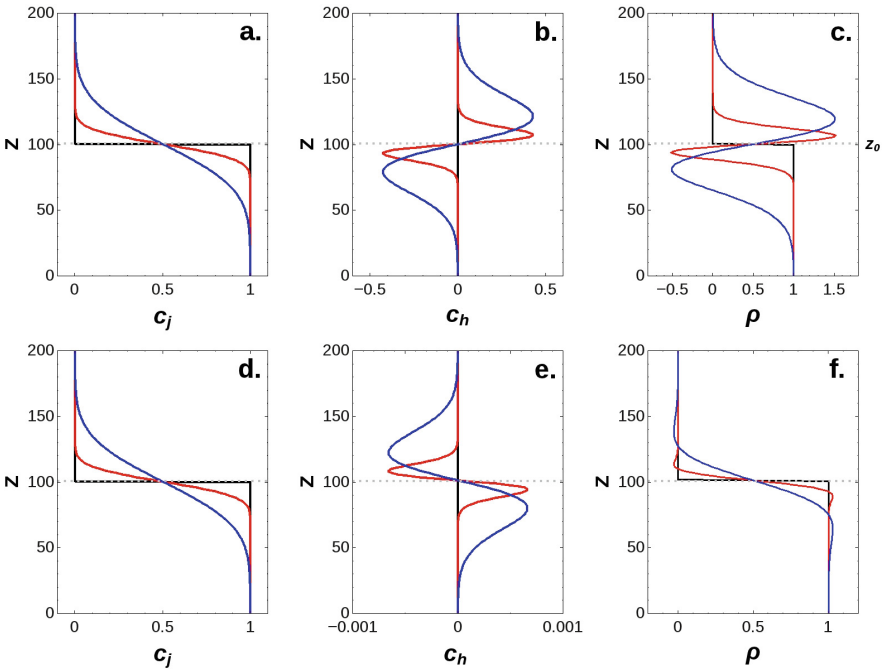


**Fig. 3.** Typical spatio-temporal evolution of the dimensionless concentration profiles  $c_j(z, \tau)$  and  $c_h(z, \tau)$  when  $\delta_{hj} > 0$  (4.70) (panels (a) and (b)) or  $\delta_{hj} < 0$  ( $-0.01$ ) (panels (d) and (e)); panels (c) and (f) show the corresponding dimensionless density profiles computed by means of Eq. 3, with  $R = 0.5$  and  $100$ , respectively. In each panel black lines describe the initial distribution of the species, while red and blue profiles depict the spatial concentrations at successive times (Colour figure online).

quantifies the relative weight of the initially homogeneous species,  $h$ , to the global density with respect to species  $j$ , featuring the initial concentration jump. In Eq. (3),  $\alpha_j = \frac{1}{\rho^T} \frac{\partial \tilde{\rho}}{\partial C_j}$  and  $\alpha_h = \frac{1}{\rho^T} \frac{\partial \tilde{\rho}}{\partial C_h}$  the solutal contributions of the species  $j$  and  $h$ , respectively, to the dimensional density  $\tilde{\rho}$ .

When the contribution to the density of the initially homogeneous species is dominant, the shape of  $c_h(z, \tau)$ , will be reflected in the spatio-temporal evolution of the density profile  $\rho(z, \tau)$ . Under the action of the gravitational field, non-monotonic density profiles are at the basis of convective instabilities (see Fig. 3(c) and (f)), whereby denser areas of a fluid locally overlies less dense zones.

By analyzing the morphology of a density profile along the gravitational axis we can, thus, predict conditions for the onset of cross-diffusion-driven hydrodynamic instabilities together with the topology of the resulting patterns [2, 3, 23]. In recent work [1], it has been demonstrated that conditions for a convective instability are met when

$$R > \frac{\sqrt{\delta_{hh}}(1 + \sqrt{\delta_{hh}})}{|\delta_{hj}|} \quad (5)$$

and the sign of  $\delta_{hj}$  discriminates the domains where Positive Cross-Diffusion-Driven Convection, **PCC** scenarios ( $\delta_{hj} > 1$ ) or Negative Cross-diffusion-driven Convection, **NCC** scenarios ( $\delta_{hj} < 1$ ) are to be expected. In particular, in PCC scenarios, starting from an initially stable condition in which the density increases downwards the gravitational axis, the density profile changes in time developing a density maximum overlying a density depletion area across the initial interface between the two layers. This results in a fingered deformation of the interface, like in the classical double diffusion (DD) instability [5, 23]. NCC profile is reminiscent of typical density profiles characterizing diffusive layer convection (DLC) scenarios where convective modes grow in the upper and the lower layer, without deforming the initial contact line between the two stratified solutions [5, 23].

In order to confirm the theoretical results obtained from the density-profile-based analysis and to obtain a spatio-temporal picture on the cross-diffusion-driven convection phenomenology, it is necessary to solve the full nonlinear problem in which Fickian equations are coupled to Stokes equations (for details see [1]):

$$\partial_\tau c_j + (\mathbf{v} \cdot \nabla) c_j = \nabla^2 c_j + \delta_{jh} \nabla^2 c_h \quad (6)$$

$$\partial_\tau c_h + (\mathbf{v} \cdot \nabla) c_h = \delta_{hj} \nabla^2 c_j + \delta_{hh} \nabla^2 c_h \quad (7)$$

$$\nabla p = \nabla^2 \mathbf{v} - (R c_h + c_j) \mathbf{1}_z \quad (8)$$

$$\nabla \cdot \mathbf{v} = 0. \quad (9)$$

The CDC equations are derived in the dimensionless form by introducing the set of scaled variables  $\{\tau = t/t_0, (x, z) = (X, Z)/L_0, (c_j, c_h) = (C_j - C_{j,0}^T, C_h - C_{h,0}^T)/\Delta C_{j,0}, \mathbf{v} = \mathbf{V}/v_0, p = P/p_0\}$ , where the scales of the velocity  $\mathbf{v}$  and the pressure  $p$  are defined as  $v_0 = L_0/t_0$  and  $p_0 = \mu/t_0$ , respectively.

By solving Eqs. (6–9) through the Alternating Direction Implicit Method (ADI), we can obtain an overview on the dynamics of the two possible instabilities. Simulations are run by using no-flux boundary conditions for the concentration field of the chemical species at the four solid boundaries of the squared spatial domain while no-slip boundary conditions are imposed for the velocity field. Figure 4 shows the dynamical destabilization of the two-layer interface due to a PCC mechanism (panel (a)) and a typical NCC scenario (panel (b)). The snapshots illustrate the spatio-temporal evolution of the instabilities by mapping the vorticity  $\omega(x, z, \tau) = \nabla \times \mathbf{v}$  over the simulation spatial domain. In both cases, the unstable area starts from the border of the spatial domain where a numerical perturbation can break the symmetry and extends along the horizontal direction. As convective fingers form, they grow vertically along the gravitational axis. Delayed forming fingers show an apparent drifting towards the side where the instability nucleates, attracted by residual flows and progressively merge with pre-existing fingers.

The PCC scenario is induced by the positive cross-diffusion term  $\delta_{hj}$  when the buoyancy ratio  $R$  meets the requirement of Eq. (5). As previously shown in Fig. 3(a) and (b), solute  $j$  diffuses from the bottom to the upper layer due to the initial gradient and triggers a non-monotonic distribution of  $c_h(z, \tau)$ , thus inducing a local density maximum over a minimum downwards  $z$ , symmetrically located around  $z_0$  (Fig. 3(c)).

Again, when Eq. (5) is satisfied, a negative cross-diffusion coefficient  $\delta_{hj}$  initiates a NCC-type convective pattern. Here the motion of solute  $j$  sustains the non-monotonic concentration profile  $c_h(z, \tau)$  shown in Fig. 3(e). During the development of the instability the initial interface is not deformed because of the formation of the density maximum located below the initial interface, which acts as a density barrier preventing the finger growth from the top to the bottom layer (Fig. 3(f)).

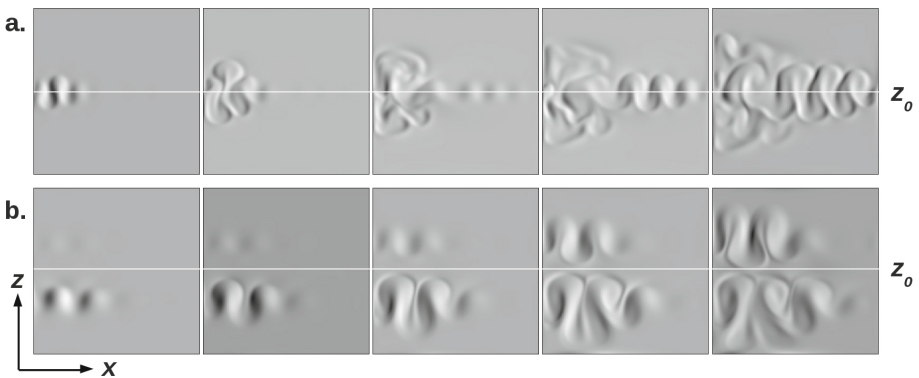


**Fig. 4.** Typical spatio-temporal evolution of a PCC (upper panel) and a NCC (lower panel) instability. The PCC scenario is obtained with  $\delta_{hj} = 4$  and  $R = 0.5$  while the NCC scenario with  $\delta_{hj} = -0.01$  and  $R = 100$ . These values are inspired from microemulsions data.

### 3 Experiments

As mentioned in the introduction, microemulsions show non-negligible cross-diffusion due to compartmentalization which can be characterised by means of the Taylor dispersion technique [2, 3, 14, 15]. In a wide range of the ME composition the diffusion matrix  $\mathbf{D}$  presents a large and positive cross-diffusivity  $D_{12}$  relating the motion of the water (species 1) to the flux of the surfactant (species 2) while a small negative cross-diffusion  $D_{21}$  quantifies the effect of water motion on AOT diffusion:

$$\mathbf{D} = \begin{pmatrix} 0.6 & 7.8 \\ -0.01 & 1.3 \end{pmatrix} \times 10^{-6} \text{cm}^2 \text{s}^{-1} \quad (10)$$

Thus, ME represent a good model to test the existence of PCC and NCC, depending on the initial gradient imposed either in the concentration of water or AOT.

The most convenient reactor for studying convective dynamics at the interface between two ME of different compositions consists of a vertically oriented Hele-Shaw cell, composed of two borosilicate glasses separated by a teflon spacer of 0.10 mm (see Fig. 5) [2, 3, 18]. Two different water-in-oil (W/O) reverse microemulsions were filled in the reactor through the inlet ports positioned at the top and the bottom of the cell. The excess of the solutions is pumped out through the cell's outlets until a flat interface between the two liquids is obtained. Each of the two microemulsions having different composition initially occupies half of the reactor height. The top and bottom solutions are prepared by using distilled

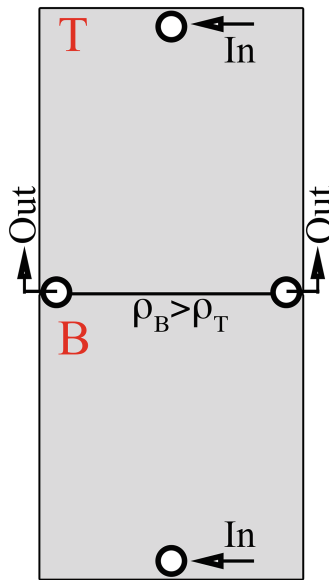
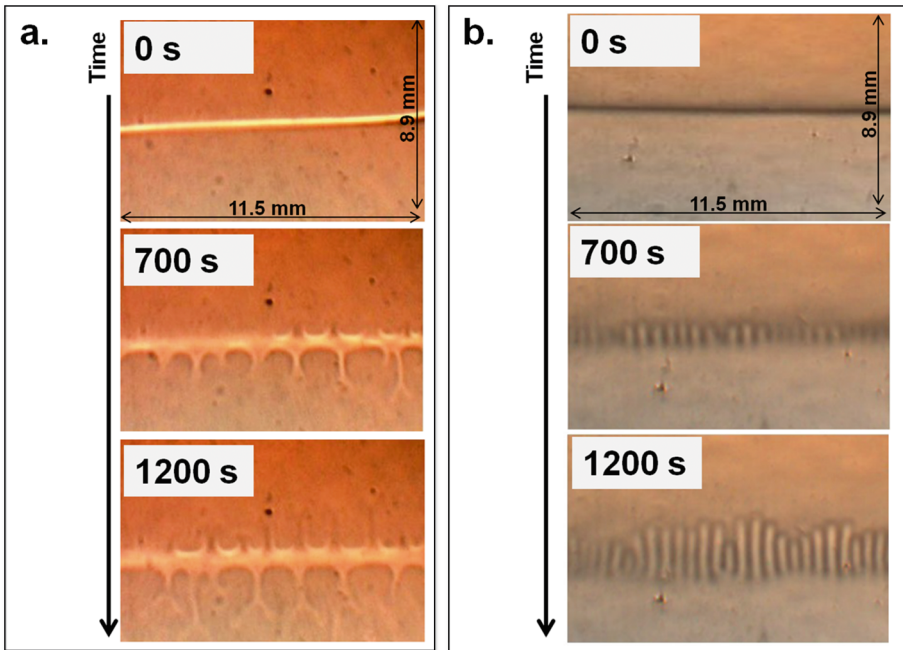


Fig. 5. Sketch of a Hele-Shaw cell.

water and a concentrated AOT in octane stock solution, conveniently diluted until the desired composition is reached. The dynamics of the interface is generally monitored by using a schlieren technique [17], which allows to observe the gradients in the refractive index between the two microemulsions, due to their density differences and, therefore, monitor the convective motions in solutions without the presence of dyes.

In all experiments the ME located in the bottom is denser than the one on the top, thus the system is initially stable towards buoyantly driven instabilities. Thanks to the presence of a negative and a positive cross-diffusion term, we can explore both the negative (NCC) and positive (PCC) cross-diffusive-driven instability by imposing a concentration jump in water or AOT, respectively. For the negative cross-diffusive case, theoretically described by the Fig. 3(d-f) and Fig. 4(b), the two ME are prepared as to have [AOT] initially constant everywhere, while the ME on the top has less water than that placed below. For a certain range of  $\Delta H_2O$ , depending on the experimental conditions, the initially stable configuration becomes unstable after few minutes from the beginning of the experiment. As an example, Fig. 6(a) shows the appearance of convective vortices localized in the top and in the bottom layer at symmetric distances



**Fig. 6.** Typical examples of cross-diffusion-driven instabilities obtained with microemulsions. (a) Three snapshots taken at  $t = 0, 700$  and  $1200$  s displaying the evolution of the NCC mode obtained with  $\Delta H_2O_{\text{bottom-top}} \simeq 1$  M. (b) The PCC scenario is obtained with  $\Delta AOT_{\text{bottom-top}} \simeq 0.05$  M.

above and below the unperturbed interface, when  $\Delta H_2O \simeq 1$  M. This compares favourably with the classification and the spatio-temporal dynamics shown in the theoretical section.

In order to induce a positive cross-diffusive-driven convective instability, theoretically described by the Fig. 3(a–c), the initial composition of the two ME has to be the other way around respect to the NCC case:  $[H_2O]$  is constant throughout the upper and the lower layers, while  $[AOT]$  is larger in the bottom ME.

Again, for a certain interval of  $\Delta[AOT]$  the interface between the two ME can be destabilised, and in this case it deforms into fingers that grow vertically and symmetrically with time across the interface (see Fig. 6(b)). These structures are successfully predicted by the analysis of the density profile obtained from the cross-diffusion model in analogous conditions and the phenomenology favourably compares with nonlinear simulations.

As a proof of concept, the PCC scenario has also been investigated in microemulsions when a further solute is dissolved in the water core of the bottom solution. It was shown, in fact, that water-soluble molecules, when dissolved in ME, induce a large and positive co-flux both in the AOT and in the  $H_2O$  [15]. Figure 7 shows the appearance of convective fingers, which grow upwards and downwards around the interface, in a system where  $KMnO_4$  has been added to

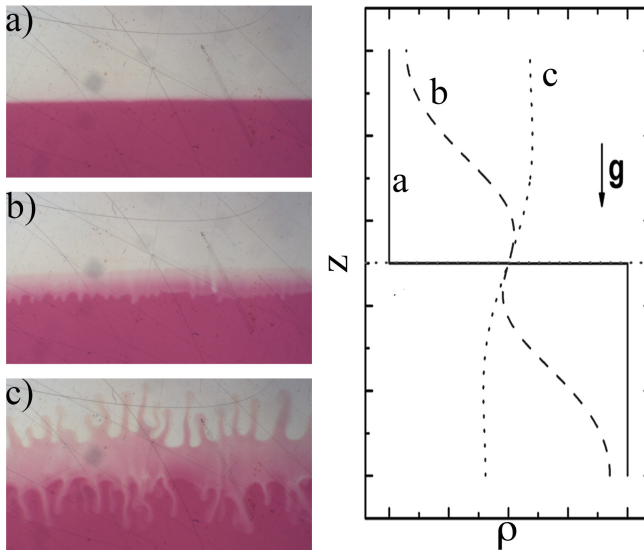


**Fig. 7.** Panels (a)–(c) show the spatio-temporal evolution of the interface between two stratified identical MEs, where the bottom one also contains the water soluble species  $KMnO_4$ . The snapshots are taken at 0, 300 and 600 s after the beginning of the experiment, respectively. The panel on the right describes the evolution of the density profile obtained by solving the diffusion Eqs. (1–2) for a 3-components system. The profiles a, b, c in the right panel describe the density distribution along the gravitational axis at the time corresponding to panels (a), (b) and (c), respectively.

the bottom ME. The composition of the two ME is such that no gradients are present in the concentrations of the water and the surfactant; in this configuration the interface is initially stable since the bottom solution is denser than the top one (Fig. 7(a)). However, the flux of  $\text{KMnO}_4$  triggers the motion of a large quantity of  $\text{H}_2\text{O}$  and AOT molecules since both cross-diffusion terms are large and positive. Therefore, when  $\text{KMnO}_4$  diffuses from the bottom to the upper layer, it drags along both  $\text{H}_2\text{O}$  and AOT molecules thus generating a non-monotonic density distribution around the contact line, destabilising the initially stable system (Fig. 7(b) and (c)). Even in this case, the evolution of the density profile has been reconstructed by integrating the Fickian Eqs. (1–2) for a 3-components system and combining it to the state Eq. (3). The resulting graph depicted in the right panel of Fig. 7 shows how the system undergoes a typical PCC scenario.

## 4 Conclusions

In this work we have presented a proof of concept that, by inducing convective transport, cross-diffusion can promote an efficient way to transport of spatio-temporal information in response to specific chemical gradients. We have shown how cross-diffusion-driven convection can be isolated and controlled in double-layer stratifications in the gravitational field. Furthermore, the resulting instability scenarios have been described in a general theoretical framework. Numerical results have been validated by means of experiments carried out with microemulsions which represent an ideal model system to investigate the two possible convective patterns, being characterized by a positive and a negative off-diagonal term in the cross-diffusion matrix.

Microemulsions also feature a convenient dispersed medium in this context because they have been widely studied in combination with chemical reactions. This paves the avenue to new chemo-hydrodynamic pattern formation and to unravel how cross-diffusion-driven convection interacts with linear and nonlinear chemical kinetics.

Future challenges are to engineer the results of this study to issues of applied interest, for instance in the realm of pollutant remediation processes and drug delivery.

**Acknowledgments.** F.R. was supported by the grant ORSA149477 funded by the University of Salerno (FARB ex 60 %) and gratefully acknowledges the support through the COST Action CM1304 (Emergence and Evolution of Complex Chemical Systems). M.A.B. gratefully acknowledges Regione Sardegna for financial support in the framework of “Asse IV Capitale Umano, Obiettivo Operativo I.3 Linea di Attività I.3.1 del P.O.R. Sardegna F.S.E. 2007/2013 - Progetti in forma associata e/o partenariale C.U.P. E85E12000060009” and the European Space Agency (ESA) Topical Team on “Chemo-Hydrodynamic Pattern Formation at Interfaces”.

## References

1. Budroni, M.A.: Cross-diffusion-driven hydrodynamic instabilities in a double-layer system: general classification and nonlinear simulations. *Phys. Rev. E* **92**(6), 063007 (2015)
2. Budroni, M.A., Carballido-Landeira, J., Intiso, A., De Wit, A., Rossi, F.: Interfacial hydrodynamic instabilities driven by cross-diffusion in reverse microemulsions. *Chaos Interdisc. J. Nonlinear Sci.* **25**(6), 064502 (2015)
3. Budroni, M.A., Lemaigre, L., De Wit, A., Rossi, F.: Cross-diffusion-induced convective patterns in microemulsion systems. *Phys. Chem. Chem. Phys.* **17**(3), 1593–1600 (2015)
4. Budroni, M.A., Rossi, F.: A novel mechanism for in situ nucleation of spirals controlled by the interplay between phase fronts and reaction diffusion waves in an oscillatory medium. *J. Phys. Chem. C* **119**(17), 9411–9417 (2015)
5. Carballido-Landeira, J., Trevelyan, P.M.J., Almarcha, C., De Wit, A.: Mixed-mode instability of a miscible interface due to coupling between Rayleigh-Taylor and double-diffusive convective modes. *Phys. Fluids* **25**(2), 024107 (2013)
6. Epstein, I.R.: Coupled chemical oscillators and emergent system properties. *Chem. Commun.* **50**(74), 10758–10767 (2014)
7. Epstein, I.R., Vanag, V.K., Balazs, A.C., Kuksenok, O., Dayal, P., Bhattacharya, A.: Chemical oscillators in structured media. *Acc. Chem. Res.* **45**(12), 2160–2168 (2011)
8. Ganguli, A.K., Ganguly, A., Vaidya, S.: Microemulsion-based synthesis of nanocrystalline materials. *Chem. Soc. Rev.* **39**(2), 474–485 (2010)
9. Leaist, D.G.: Relating multicomponent mutual diffusion and intradiffusion for mass-associating solutes. Application to coupled diffusion in water-in-oil microemulsions. *Phys. Chem. Chem. Phys.* **4**(19), 4732–4739 (2002)
10. Leaist, D., Hao, L.: Size distribution model for chemical interdiffusion in water AOT Heptane water-in-oil microemulsions. *J. Phys. Chem.* **99**(34), 12896–12901 (1995)
11. Rossi, F., Budroni, M.A., Marchettini, N., Carballido-Landeira, J.: Segmented waves in a reaction-diffusion-convection system. *Chaos Interdisc. J. Nonlinear Sci.* **22**(3), 037109 (2012)
12. Rossi, F., Liveri, M.L.T.: Chemical self-organization in self-assembling biomimetic systems. *Ecol. Model.* **220**(16), 1857–1864 (2009)
13. Rossi, F., Ristori, S., Marchettini, N., Pantani, O.L.: Functionalized clay microparticles as catalysts for chemical oscillators. *J. Phys. Chem. C* **118**(42), 24389–24396 (2014)
14. Rossi, F., Vanag, V.K., Epstein, I.R.: Pentanary cross-diffusion in water-in-oil microemulsions loaded with two components of the Belousov-Zhabotinsky reaction. *Chem. Eur. J.* **17**(7), 2138–2145 (2011)
15. Rossi, F., Vanag, V.K., Tiezzi, E., Epstein, I.R.: Quaternary cross-diffusion in water-in-oil microemulsions loaded with a component of the Belousov-Zhabotinsky reaction. *J. Phys. Chem. B* **114**(24), 8140–8146 (2010)
16. Rossi, F., Zenati, A., Ristori, S., Noel, J.M., Cabuil, V., Kanoufi, F., Abou-Hassan, A.: Activatory coupling among oscillating droplets produced in microfluidic based devices. *Int. J. Unconventional Comput.* **11**(1), 23–36 (2015)
17. Settles, G.S.: *Schlieren and Shadowgraph Techniques*. Springer, Berlin (2001)
18. Shi, Y., Eckert, K.: A novel Hele-Shaw cell design for the analysis of hydrodynamic instabilities in liquid systems. *Chem. Eng. Sci.* **63**(13), 3560–3563 (2008)

19. Taylor, A.F., Tinsley, M.R., Wang, F., Huang, Z., Showalter, K.: Dynamical quorum sensing and synchronization in large populations of chemical oscillators. *Science* **323**(5914), 614–617 (2009)
20. Tomasi, R., Noel, J.M., Zenati, A., Ristori, S., Rossi, F., Cabuil, V., Kanoufi, F., Abou-Hassan, A.: Chemical communication between liposomes encapsulating a chemical oscillatory reaction. *Chem. Sci.* **5**(5), 1854–1859 (2014)
21. Tompkins, N., Li, N., Girabawe, C., Heymann, M., Ermentrout, G.B., Epstein, I.R., Fraden, S.: Testing Turing's theory of morphogenesis in chemical cells. *Proc. Natl. Acad. Sci.* **111**(12), 4397–4402 (2014)
22. Torbensen, K., Rossi, F., Pantani, O.L., Ristori, S., Abou-Hassan, A.: Interaction of the Belousov-Zhabotinsky reaction with phospholipid engineered membranes. *J. Phys. Chem. B* **119**(32), 10224–10230 (2015)
23. Trevelyan, P.M.J., Almarcha, C., De Wit, A.: Buoyancy-driven instabilities of miscible two-layer stratifications in porous media and Hele-Shaw cells. *J. Fluid Mech.* **670**, 38–65 (2011)
24. Vanag, V.K.: Waves and patterns in reaction-diffusion systems. Belousov-Zhabotinsky reaction in water-in-oil microemulsions. *Physics-Uspokhi* **47**(9), 923–941 (2004)
25. Vanag, V.K., Epstein, I.R.: Pattern formation in a tunable medium: the Belousov-Zhabotinsky reaction in an aerosol OT microemulsion. *Phys. Rev. Lett.* **87**(22), 228301–228304 (2001)
26. Vanag, V.K., Epstein, I.R.: Cross-diffusion and pattern formation in reaction-diffusion systems. *Phys. Chem. Chem. Phys.* **11**(6), 897–912 (2009)
27. Zemskov, E.P., Kassner, K., Hauser, M.J.B., Horsthemke, W.: Turing space in reaction-diffusion systems with density-dependent cross diffusion. *Phys. Rev. E* **87**(3), 032906 (2013)